Exp Brain Res (1994) 101:8–23

ORIGINAL PAPER

Longtang L. Chen · Lie-Huey Lin · Edward J. Green
Carol A. Barnes · Bruce L. McNaughton

Head-direction cells in the rat posterior cortex

I. anatomical distribution and behavioral modulation

Received: 4 January 1993 / Accepted: 1 February 1994

Abstract We examined the behavioral modulation of head-directional information processing in neurons of the rat posterior cortices, including the medial prestriate (area Oc2M) and retrosplenial cortex (areas RSA and RSG). Single neurons were recorded in freely moving rats which were trained to perform a spatial working memory task on a radial-arm maze in a cue-controlled room. A dual-light-emitting diode (dual-LED) recording headstage, mounted on the animals' heads, was used to track head position and orientation. Planar modes of motion, such as turns, straight motion, and nonlocomotive states, were categorized using an objective scheme based upon the differential contributions of movement parameters, including linear and angular velocity of the head. Of 662 neurons recorded from the posterior cortices, 41 head-direction (HD) cells were identified based on the criterion of maintained directional bias in the absence of visual cues or in the dark. HD cells constituted 7 of 257 (2.7%) cells recorded in Oc2M, 26 of 311 (8.4%) cells in RSA, and 8 of 94 (8.5%) cells in RSG. Spatial tuning of HD cell firing was modulated by the animal's behaviors in some neurons. The behavioral modulation occurred either at the preferred direction or at all directions. Moreover, the behavioral selectivity was more robust for turns than straight motions, suggesting that the angular movements may significantly contribute to the head-directional processing. These behaviorally selective HD cells were observed most frequently in Oc2M (4/7, 57%), as only 5 of 26 (19%) of RSA cells and none of the RSG cells showed behavioral modulation. These data, taken together with the anatomical evidence for a cascade of projections from Oc2M to RSA and thence to RSG, suggest that there may be a simple association between movement and head-directionality that serves to transform the egocentric movement representation in the neocortex into an allocentric directional representation in the periallocortex.

Key words Single units · Head direction · Behavior
Neocortex · Retrosplenial cortex

L.L. Chen[1] (✉) · L.-H. Lin · E.J. Green
Behavioral Neuroscience Program, University of Colorado, Boulder, CO 80309, USA
FAX no. (81) 48-462-4696, e-mail: lt@murasaki.riken.go.jp

C.A. Barnes · B.L. McNaughton
ARL Division of Neural System, Memory and Aging, University of Arizona, Tucson AZ 85724, USA

Present addresses:
[1] Laboratory for Neural Information, RIKEN, 2-1, Hirosawa, Saitama 351-01, Japan
[2] Laboratory of Neurogenetics, NIAAA, 12501 Washington Ave, Rockville, MD 20852; USA
[3] Department of Psychology, University of Miami, Coral Gables, FL 33146, USA

Introduction

Head-direction (HD) cells were first found in the postsubiculum by Ranck (1984). These cells were named after their firing characteristic which was simply a function of the horizontal component of animals' head directions, irrespective of location and behaviors. Moreover, HD cells showed visual modulation, in that these cells shifted their preferred directions according to shifts of a prominent environmental stimulus, such as a cue-card on the wall of a dimly lighted recording apparatus (Taube et al. 1990a). The directional characteristics, however, persisted after the cue-card was removed, thus distinguishing HD cells from cells with simple sensory correlates, such as those found in the visual cortex.

Preliminary work from this laboratory indicates that some cells in the rat posterior parietal cortex (the rostral medial prestriate, Oc2M) and the posterior cingulate (also called the retrosplenial cortex in rats) also show strong directional preferences (Chen and McNaughton 1988; Green and McNaughton, unpublished). These cells, having properties similar to the postsubicular HD cells, exhibit persistent directional activity in total darkness and are not necessarily dependent upon simple sen-

sory stimuli. However, unlike most of the postsubicular HD cells, the cells observed in our study were movement sensitive; activity of these cells was modulated by behavioral modes. Thus, a careful examination of the behavioral modulation of posterior parietal and retrosplenial HD cells may provide insights into understanding the function of HD cells in the processing of directional information.

Neurophysiological studies in primates have found that the posterior parietal cortex plays an important role in directional information processing (Mountcastle et al. 1975; Hyvarinen 1982; Andersen et al. 1985, Andersen 1987). Posterior parietal neurons, however, code for egocentric (head-centered) coordinates, i.e., the activity is modulated by both retinotopic location and eye position (Zipser and Andersen 1988). These findings suggest that posterior parietal cortex, a homolog of Oc2M in rats, plays a role in integrating an external sensory organ-dependent (i.e., retina-centered) coordinate with an internally generated movement coordinate (i.e., eye position in the orbit). Thus, one objective of the present study was to assess whether movement information is involved in the directional processing of HD cells in the Oc2M and the adjacent areas which bridge between the posterior parietal cortex and the postsubiculum, the retrosplenial cortex (dysgranular, RSA, and granular RSG; Zilles 1985). We developed an objective categorization scheme using information derived from a dual-light-emitting diode (dual-LED) tracking apparatus, in order to categorize different behavioral modes. In addition, simultaneous recordings from groups of cells using the stereotrode technique (McNaughton et al. 1983) has provided initial information regarding the functional organization of HD cells in these cortical areas. The accompanying paper (Chen et al. 1994) describes the control of visual cues and ideothetic cues over these HD cells. Some preliminary results from these experiments have been presented in abstract form (Chen et al. 1990, 1991).

Materials and methods

Subjects and implantation of recording electrodes and cylinders

Fifteen male Fisher-344 rats, obtained from Charles River breeding colonies, were used in this study. These animals, aged between 10 and 15 months through the period of the experiment, were housed in individual cages, with the animal room maintained on a 12-h light-12-h dark cycle. Their body weights were maintained at approximately 80% of the free-feeding weight during initial training. These animals were surgically prepared under deep anesthesia (30 mg/kg pentobarbital sodium, Nembutal, i.p.) before training. The surgical procedures conformed to the requirements of the National Institutes of Health (NIH) guidelines for laboratory animals.

Eight experimental animals were implanted with recording electrodes that were permanently attached to microdrives capable of movement in the dorsoventral plane, while seven others were implanted with recording cylinders (3.4 mm in inner diameter, 8 mm in height) in which electrodes could be replaced and/or repositioned as necessary. Both microdrives and cylinders were manufactured in this laboratory. The coordinates of recording sites were within an area of 2–6.5 mm A-P and 0–4.5 mm M-L, based on the corresponding stereotaxic coordinates (Zilles 1985). Small holes were drilled in the skull for the placement of recording electrodes and anchor screws. The space between the dura and the skull surface was filled with a layer of plastic (RTV Silastic; Dow Corning), and the dura remained intact. The space of the cylinder was filled with bone-wax, through which the electrodes could be advanced. Reference electrodes were teflon-coated stainless-steel wires (114 μm in diameter) inserted into the space between the skull and the dura. Similar wires, attached to jewelers' screws and implanted into the skull, served as ground wires. Both the reference and the ground wires were crimped to male amphenol pins and socketed into a nine-hole cylindrical connector, which was then cemented behind the microdrives and cylinders.

After the animals recovered from surgery and regained their free-feeding body weights, they were food-restricted to about 90% of their free-feeding weight, and subjected to retraining. It took 4–5 weeks to complete the task training for each animal.

Behavioral tasks and cue-controlled environment

The rats were trained to perform a spatial working memory task on a radial eight-arm maze. For simplicity, the spatial working memory task will sometimes be referred to as the maze task. The maze was located at the center of a 360 × 360-cm room. The maze consisted of eight arms (6 × 60 cm) and a central platform (20 cm in diameter). The maze was elevated 80 cm from the ground. A small aluminum container was placed at the end of each arm. The containers were baited with chocolate milk (approximately 0.3 ml) once per trial during recording. A d.c. motor-controlled joint situated beneath the midpoint of each arm allowed the near-center ends of the maze arms to be lowered so that the arms would be inaccessible to the animals during part of the task.

The spatial working memory task (Olton and Samuelson 1976) started with the experimenter baiting each arm while the animals were confined in a rubber tray (20 cm) in the maze center. The task consisted of two phases: a sampling phase and a memory phase. In the sampling phase, four randomly assigned arms were accessible to the animals. As soon as the animals approached the last arm, the other arms were raised; this signaled the beginning of the memory phase, during which the animals had to visit the rest of the arms to obtain further rewards. When the animals visited the last arm and ran back to the center, they were replaced into the rubber tray. This signaled the intertrial interval. Because each arm was baited once per trial, animals were reinforced to choose the arms which they had not visited previously in each trial. An overtrained animal could perform the task with very few or no mistakes. It took about 2–4 min (including 40–60 s of intertrial interval) for a trained animal to finish one trial.

Two types of behavioral experiments were conducted. For the first (six) rats, the maze room was painted light green, and numerous pieces of equipment and other spatial cues were distributed around the room. The only salient and manipulable visual cue was the room light (60 W incandescent), which was hung on the wall, elevated 150 cm from the ground. The animals performed the spatial working memory task, and their position was monitored using a single-LED tracking method (see below). For the second group of (nine) rats, the maze room was painted entirely flat black and was illuminated by a single 40-W reflector light bulb on the center of the ceiling at a distance of 250 cm from the maze surface. The light bulb was enclosed in a cardboard cylinder so that it would only light the radial-arm maze and the floor underneath. The illuminance of the wall was no more than 1 cd/m^2. Four 60 × 90-cm cardboard panels, one white and three black, were used as controlled visual cues. These panels were placed symmetrically on the four sides (i.e., north, east, south, and west) of the room, standing right above the maze surface, approximately 15 cm away from the arm-ends. The white panel was the brightest spatial object in the room; its illuminance was approximately 5 cd/m^2. The illuminance of the black panels was about half of that of the white panel. The experimenter, wearing a black lab

coat, was seated behind one of the panels in the maze task, from where he could monitor the animal's movement through the shadow cast on the floor.

Head position and head-direction tracking and analyses

The video image of the animal's position was signaled by two arrays of infrared LEDs (3 mm in diameter) which were mounted on each end of a 13- or 21-cm rod attached to the recording headstage (see Fig. 3A). The larger diode array was located at the front, whereas a single LED was at the rear. Head positions and directions were obtained simultaneously from the front-LED positions and the front-back-LED alignments, respectively. The multiple-spot tracking system (BrainWave Systems) consisted of a CCD camera (Pulnix America) and a camera tracker interface (SA-2 Tracker;, BrainWave Systems) that was connected to a 24-bit PIO parallel inferface board in the BrainWave Systems computer. The basic principle was to detect and discriminate two bright points based upon their sizes. The scanned field covered 255×244 pixels, with each pixel corresponding to an area approximately 6.5×6.5 mm on the maze surface. The center coordinates of the front and back LED arrays were computed based on the averaged coordinates of the first and the last scanned points within 7-pixel radius, and the position data were time stamped and stored at a rate of 20 Hz. In the first design of the headstage, the front LED array (12×15 mm) consisted of 8 LEDs with the long axis aligned with the front-rear direction, the distance between the front and the back LED arrays was 21 cm. In the second design, the front LED array consisted of two LEDs (12 mm apart) with the long axis aligned with the front-rear direction; the distance between the front and the back LED arrays was 13 cm. These designs resulted in an head direction resolution of $\pm 3.5°$ (for the first design) and $\pm 2.0°$ (for the second design), respectively, measured when the recording headstage was presented at nine spots (the center and eight arm-ends) of the maze with the recording cable swag across the recording headstage. Note that the intrinsic tracking error of the system was 6.5 cm/s, given that the dimension of each pixel was 6.5×6.5 cm and the sampling rate was 20 Hz. The latter design was used in most of the experiments reported in this paper. There were two possible circumstances under which the LED coordinates could be either reversed or missing, leading to errors in head direction. The first involved an improper determination of the size of an LED array, which could be due to a partial blockade of the LED image by recording cables. The second was the "fusion" of the front and back LED arrays, resulting from the animal's movement in the pitch or roll planes. To circumvent these problems, a user-interactive video-display was employed, allowing the experimenter to visualize the continuity of the position coordinates and the corresponding head directions in the time-series of the original data record. On average, less than 5% of the data points were missampled or reversed in head directions. These imperfections were corrected using several computational algorithms developed in this laboratory. The coordinates of the missampled points were either linearly interpolated (for those missampled by no more than 500 ms) in postacquisitional analysis or left out of the subsequent analyses. On average, about 1% of the total data points were truly missampled.

The instantaneous (either linear or angular) velocity of each position was calculated by the distance (or angles) 50 ms before and after that particular observation. The velocity (V_w) of each data point was further smoothed by weighting its unweighted velocity (v_0) and those of the preceding (v_{-1}) and succeeding (v_{+1}) points, based on the algorithm: $V_w = 12.5\%(v_{-1}) + 75\%(v_0) + 12.5\%(v_{+1})$. The purpose of smoothing the velocity data was to get rid of the "noise" that might result from the resolution limitation of the tracking system, for example, division of space into pixels. Note that the weighted velocity is the same as the non-weighted one in a constant velocity case.

The single-LED tracking method was used in the first six rats, whereas the dual-LED tracking system was used in the second nine rats. Both methods were based on the similar principle, tracking infrared images. The single-LED tracking system consisted of a RETICON tracking system (Wieland and Eaton 1983), which sampled positions 20 times per second, and a PDP 11/12 computer to record position and spike data. The resolution of the RETICON system was only up to 1.8×1.8 cm/pixel. The maze surface was divided into 100×100 such pixels.

Stereotrode recording method

The stereotrode recording method (McNaughton et al. 1983) was used to simultaneously record and discriminate action potentials from a number of neurons. The principle of this method was to discriminate units based on the differential spike parameters of inputs from different channels using a dual-channel recording electrode. This method has proven to be very useful in recording single neurons from freely moving animals and frequently enables the same units to be consistently held for several days. Unit isolation was carried out independently of the subsequent analyses of behavioral, visual, and directional correlates. Cells recorded were often isolated based upon clearly defined spike height or width, recorded from each channel. Each unit, separated from each other, formed its distinctive sets of cluster boundaries in each spike parameter. The parameters used included peak amplitude, valley amplitudes, peak phase angle, valley phase angle, spike amplitude, spike width, X-Y peak time, and X-Y latency difference, from either X or Y channels. The cluster boundaries were examined in three different portions (beginning, middle, and end) of the data in order to assess the reliability of the spike parameters of any given unit. Even when units were unstable and the spike height changed in the course of recording, the other spike parameters of the units often remained consistent so that a clear isolation was still possible. When units were small (e.g., spike heights less than 50 μV) or their spike parameters dramatically changed in the course of recording, the isolation became difficult. These units were not included in the analyses.

Two types of stereotrodes were used, one consisted of two thin, lacquer-coated tungsten wires (20 μm in bare diameter, California Fine Wire) and the other consisted of two stiff tungsten wires (100 μm in diameter, Sylvania Chemical/Metals). The two wires, insulated individually, were twisted and glued together with two electrode tips separated apart by 15–20 μm. The electrode tips were electroplated with gold to give a final impedance of 300–700 kΩ. The thin-wire stereotrodes were threaded in a 30-gauge cannula, with 2 mm protruding out of the end, and were implanted 50–100 μm below the dura during the surgery. The stiff-wire stereotrodes were threaded in a 24-gauge cannula, with 5 mm protruding out of the end, and were mounted on the microdrive before use.

Two types of microdrives were manufactured in this laboratory, used for fitting the two types of stereotrodes described above. For the thin-wire stereotrodes, each microdrive consisted of a piece of amphenol strip (as an electrode carrier) and two threaded advancing-rods (350 μm in pitch). The threads on the lower ends of the rods were ground off and 4–5 parallel circular grooves were cut in their place. This allowed the rods to rotate freely in a dental acrylic base, without linear movement. The upper ends were machined to form a flat surface, allowing for turning using a hemostat. This type of microdrive weighed about 1 g. For the stiff-wire stereotrodes, each microdrive consisted of a piece of amphenol strip, two smooth-surface supporting rods, one threaded advancing-rod, and a brass-collar base. The stereotrodes were mounted on a rotatable electrode carrier (a brass screw, 3 mm in diameter, fit into an acrylic carriage which was attached to the amphenol strip), such that the electrode positions would be rotated concentrically as necessary. This microdrive weighed approximately 4 g.

The recording setup included a two-channel, field-effect-transistor (FET) source follower mounted on the animal's head, a nine-channel commutator (Josef Biela Engineering), a set of Grass preamplifiers (model P511), a set of Neurolog filters (Neurolog System; Digitimer), an analog-digital (A/D) processor, and a mi-

crocomputer (BrainWave Neuroscience Workstation; BrainWave). The two-channel FETs matched the impedance of the neural signal with the recording system. The spike signals were amplified 5 000–10 000 times with a Grass preamplifier and filtered through a band-pass filter between 600 Hz and 7 kHz. A single-unit recording program (BrainWave) was used for processing the spike data with a maximal sampling rate of 64 kHz.

Histology

Small electrolytic lesions (2 mA for 2 s, tip positive) were made at the end of some penetrations for easy identification of the recording sites. At the end of the final recording session, the animals were killed by injections of a lethal dose of pentobarbital sodium; they were then perfused intracardiacally with 0.9% saline and 10% formalin plus 10% glacial acetic acid. For most of the animals, the last recording electrodes remained in the brain during perfusion. After perfusion, the brains were submerged in 10% formalin-glacial acetic acid solution for at least 48 h. The brains were then embedded in paraffin and sectioned coronally in 12-μm-thick-slices and stained with cresyl violet. One of every five sections was stained for myelin using the Gallyas-silver staining method (Gallyas 1979; Zilles 1985).

Results

Histological results

The experimental animals were killed immediately after the recordings were completed in both hemispheres. The first (six) animals recorded using the single-LED tracking method in the initial pilot study were all implanted with thin-wire stereotrodes. The electrode tracks were all identified. In these animals, five penetrations (81 cells) were found in Oc2M, three penetrations (66 cells) were in rostral area Oc2L, and two penetrations (25 cells) were in area RSA. No penetration was found in area RSG. For these animals, the cell-penetration ratio was 16.2, 22.0, and 12.5 for areas Oc2M, Oc2L, and RSA, respectively.

Of the second group of (nine) animals recorded using the dual-LED tracking method, two were implanted with thin-wire stereotrodes and seven were recorded using stiff-wire stereotrodes. The length of time between the first and last days of recording was 1–7 weeks. The electrode tracks of the last seven animals were identified based on criteria such as small lesions, the presence of hippocampal CA1 place cells at the bottom of the penetration, or clear tracks in the cases when electrodes were left in the brain during perfusion. These electrode tracks were found in a region approximately 2.5–6.5 mm posterior to bregma and 0.0–4.5 mm lateral to midline in stereotaxic coordinates (Zilles 1985; Fig. 1). In agreement with previous reports (Motter and Mountcastle 1981; Andersen et al. 1990), we found that electrode tracks in the brain sections remained visible for about 6 weeks after recording. In total, 56 out of 86 identified electrode tracks were recorded in these animals. Data presented included only the cells whose recording sites were identified; 257 cells were in area Oc2M, 311 were in area RSA, and 94 were in area RSG. The ratio of cell-penetration was 11.68 (257:22), 12.44 (311:25) and 9.44 (85:9) for areas Oc2M, RSA, and RSG, respectively, suggesting a rather equal cell-sampling in these cortical areas for the second group of animals. It was also noted that the RSG penetrations which went through the superior sagittal sinus produced neither noticeable behavioral impairment nor overt abnormalities in histological sections.

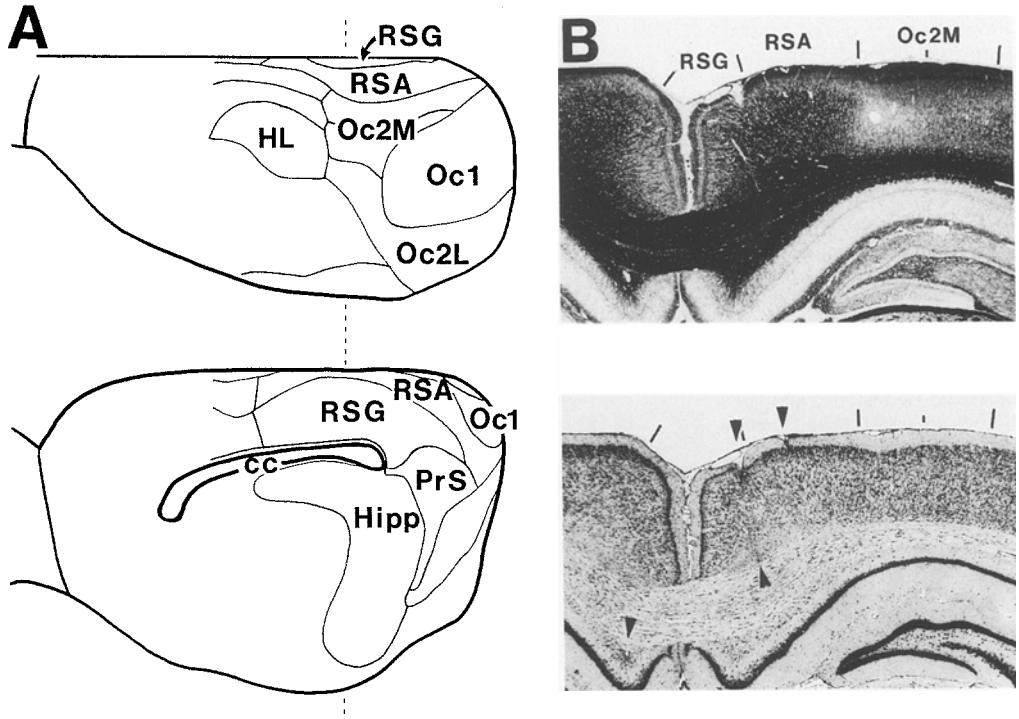

Fig. 1 **A** Line drawings of the dorsal (*top*) and medial (*bottom*) views of rat cortices. **B** Examples of identified electrode tracks in myelin- (*top*) and Nissl- (*bottom*)-stained coronal sections. The delineation of cortical areas Oc2M, RSA, and RSG is based on myeloarchitecture and cytoarchitecture (Zilles 1985). The *dashed line* (**A**) indicates the approximate rostral-caudal level from which the pictures of coronal sections were taken. Four electrode tracks are depicted by *arrowheads* (**B**). An electrolytic lesion was made just below the corpus callosum in the left hemisphere. (*cc* orpus callosum, *Hipp* hippocampus, *HL* hindlimb sensorimotor area, *Oc1* striate cortex, *Oc2L* lateral prestriate cortex, *Oc2M* medial prestriate cortex, *PrS* postsubiculum, *RSA* dysgranular retrosplenial cortex, *RSG* granular retrosplenial cortex)

Assessment of HD cell firing using single-LED tracking

There was no means of directly assessing the animal's head direction using the single-LED tracking method. However, due to the geometric restrictions of the maze, head direction could be assessed indirectly by evaluating the animal's movement direction, since the animal only traversed straight in either radially inward or outward directions in relation to the center of the maze. Figure 2 illustrates an analysis of the head-directional correlates of a HD cell recorded in the Oc2M. This cell exhibited a preference for the south direction (bottom of Fig. 2A), in which the most salient cue of the room, a 40-W incandescent light bulb, was hung on the wall. The directional tuning of the cell was most robust during straight motion and was weak in the nonlocomotive mode. The cell's activity during turns was suppressed in all directions; the suppression extended briefly in the postturn period. Such a behavioral modulation might have resulted in a reduced significance of the cell's directionality in the location near the center of the maze (e.g., the inner 6–8 bins of each arm). In order to assess the behavioral selectivity of this cell, the firing during straight motion was assessed and replotted in Fig. 2B by extracting the firing rate of the central six bins (30 cm in length) of each arm. For the straight motion, the firing rate of each direction was computed as a joined firing rate of the same direction in two opposing arms. For the nonlocomotive state, the firing rate was represented as that of the last bin of each arm in which animals stopped the forward motion and received rewards. Figure 2B shows that the cell has a broad, south-bound directional tuning for straight and nonlocomotive motions. Note

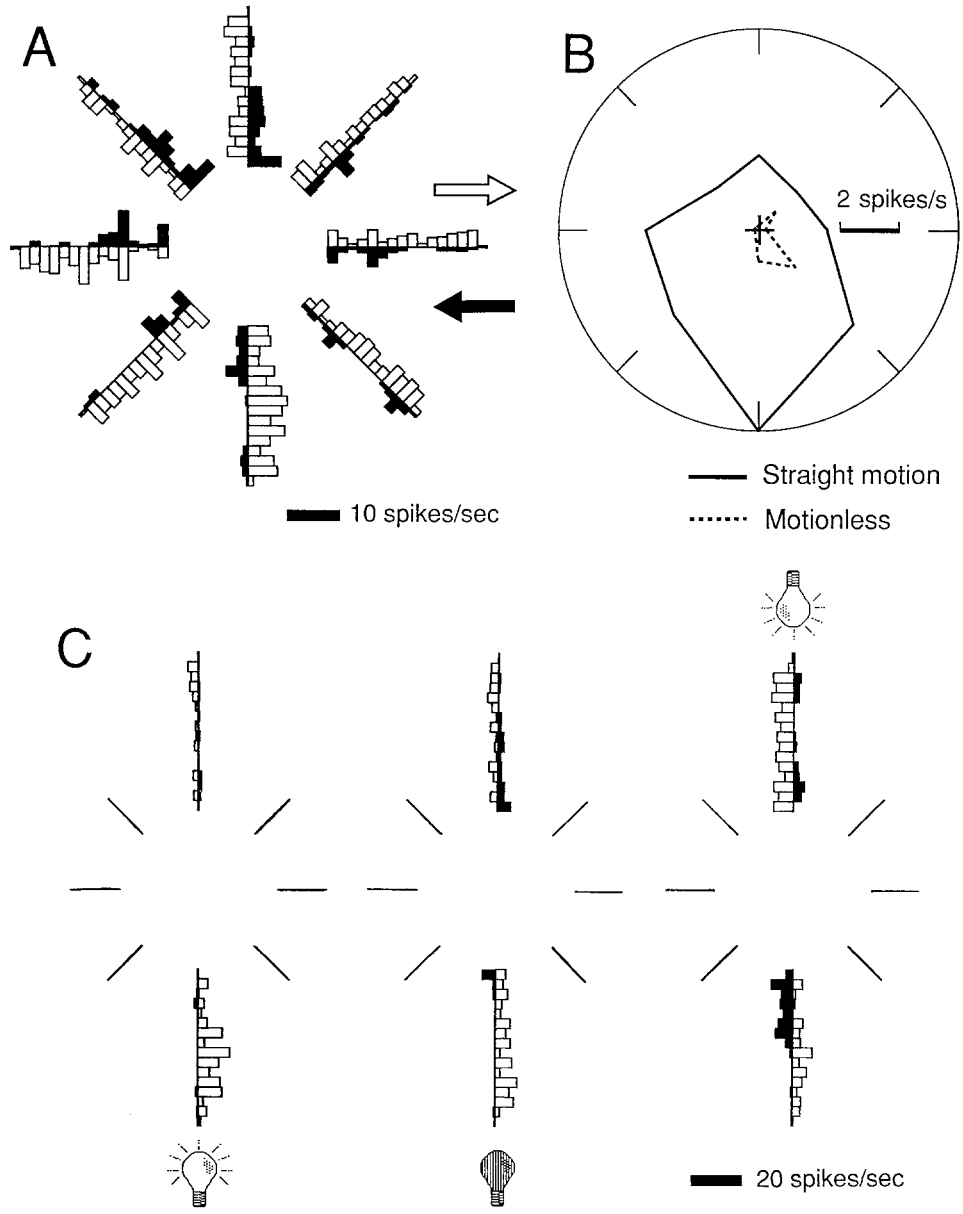

Fig. 2A–C Directional firing characteristics of a medial prestriate cortex (Oc2M) head-direction (HD) cell in the maze task, recorded using the single-light-emitting diode (LED) tracking method. The overall discharge pattern of the cell is shown in the radial histogram (**A**), in which the firing rates are separated as radially inbound (*filled bins*) versus radially outbound (*open bins*) in relation to the maze center. Each bin height represents the total number of spikes divided by the total occupancy time of the animal in that bin. The five inner bins in each radial direction correspond to parts of the central platform. The cell's directional tuning is partitioned into two behavioral modes, straight motion and nonlocomotive, in a directional tuning plot (**B**). Note that the cell activity was suppressed briefly following turns. The response of the same cell to changing the location of the light source in two-arm trials is plotted in **C**. The discharge rate of this cell increased as the animal moved out toward the light (*left*) and persisted when the light was extinguished (*middle*). When the light was moved 180° from its original location, the directional firing of this cell rotated correspondingly (*right*)

that the cell was tuned to a similar (±45°) direction, regardless of motion state.

The directional characteristics of the cell in Fig. 2 were assessed with regard to the existence of the light (or visual cues) in two-arm trials, in which the animals traversed back and forth between two arm-ends to obtain a food reward (Fig. 2C). The cell was tuned to the direction of the light (t-test, $P<0.008$), and the directional preference shifted accordingly when the location of the light was changed (t-test, $P<0.002$). This suggests that the light was an important factor in driving this cell. However, the cell's directional tuning persisted (t-test, $P<0.003$) when the south light was turned off in the transition between the two lighted periods, suggesting that the directionality of this cell did not simply result from visual stimulation. This characteristic was reminiscent of the property of postsubicular HD cells that maintained their directionality in the absence of visual inputs (Ranck 1984). We conducted the same two-arm trials to assess some of the posterior cortical neurons recorded using the single-LED tracking method. Of the neurons tested, 2 HD cells (52 tested) were identified in area Oc2M, 1 HD cell (35 tested) was in rostral Oc2L, and 1 HD cell (5 tested) was in area RSA. These HD cells all showed a preferred direction in the light, maintaining their preferred direction in total darkness, and finally shifted their preferred direction according to the shift of the major light source of the room. For all of these HD cells, behavioral states (i.e., turns, straight movement, or nonlocomotive state) significantly modulated their activities.

Quantitative analysis of head direction and behavioral categorization using dual-LED tracking

We quantitatively analyzed the head-directional and behavioral correlates of cells that were recorded using the dual-LED tracking method. In general, rats' behaviors on the maze surface can be decomposed into two planar movement parameters, head displacement (i.e., front LED displacement, Δs) and head-angle displacement (i.e., angular change of the front-back LED vector, Δθ; Fig. 3). Each movement thus can be viewed as a transitional state of motion with a particular linear and angular displacement away from the previous state of motion. When the angular velocity was small, animals were either nonlocomotive (M) or moving straight ahead with high (H) or low (O) velocity. Otherwise, animals must be making either right turns (R) or left turns (L; also see Fig. 5B). The nonlocomotive state was a behavioral state when the animals remained still or performed

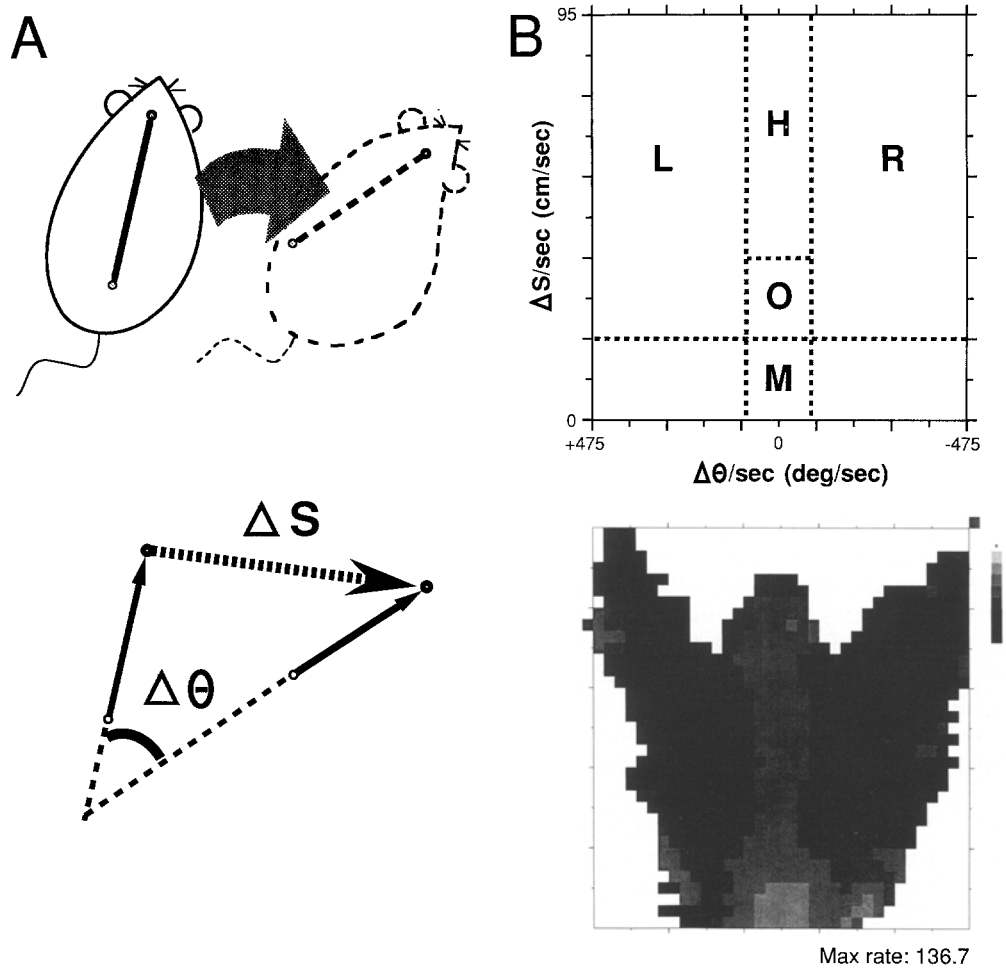

Fig. 3 Schematic drawings of the dual-light-emitting diode (dual-LED) configuration on the head of freely moving rats (**A**) and the behavioral categorization scheme used to show a cell's behavioral correlates (**B**). The relationship between the two movement parameters, head displacement (i.e., front-LED displacement, ΔS) and head-angle displacement (i.e., angular change of the front-back-LED vector, Δθ), during animal movements is illustrated in the *lower portion* of **A**. Note that the front-back-LED axis does not necessarily represent the body axis, but rather, the animal's head orientation. Based on the movement parameters the animal behaviors were categorized as nonlocomotive (*M*), right turn (*R*), left turn (*L*), high-speed straight motion (*H*), and low-speed straight motion (*O*), as in the *upper panel* in **B**. A movement-selective cell in the dysgranular retrosplenial cortex (area RSA), analyzed using this scheme, is illustrated in the *lower panel* in **B**. The firing rate of the cell is represented by eight levels of equally scaled, *gray pixels*. *Darker shades* are indicative of higher firing rates. There are at least three occurrences in each pixel; the minimal occupancy time for each occurrence was 50 ms

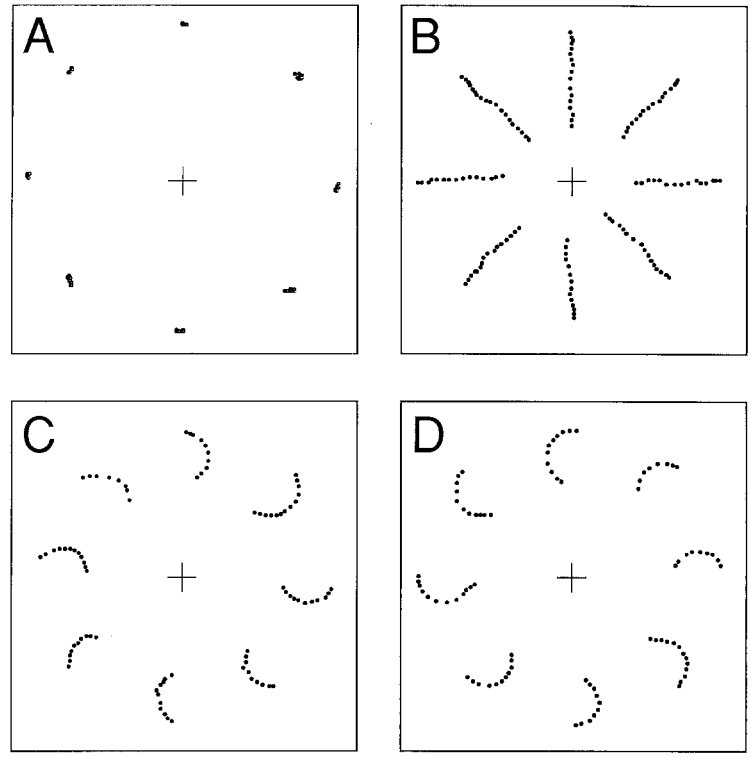

Fig. 4 Representative movement trajectories of one experimental animal showing a series of front LED positions that were separated for nonlocomotive state at the arm-ends (**A**), straight motion on eight arms (**B**), right turns at the arm-ends (**C**), and left turns at the arm-ends (**D**). *Dots* represent a series of positions sampled every 50 ms

orofacial, neck, or forelimb movements to obtain rewards in a given task or to groom themselves; thus nonlocomotion included the motionless state and slow motions, yet was distinguishable from that of high- or low-velocity movements, right or left turns. The nonlocomotive state was defined as a behavioral state with a linear velocity of less than 19 cm/s ($\Delta s/s$) and an angular velocity within $\pm 90°/s$ ($\Delta\theta/s$; also see Fig. 5A). Right turns and left turns were behavioral states with a linear velocity greater than 19 cm/s and an angular velocity whose magnitude was greater than $+90°/s$ (left) or $-90°/s$ (right). Similarly, high-velocity straight motion and low velocity were separated by a criterion of linear velocity of 38 cm/s. The resolution of the dual-LED tracking system used in these experiments was ± 2 cm/s and $\pm 25°/s$, measured at 20 Hz. Under the same conditions, the resolution of the head-directionality was $\pm 2°$.

We determined empirically the velocity cutoff for different behaviors. The onset and offset of each behavior were time-stamped as the positions of front LEDs were played back on the computer screen (Fig. 4). The animal was considered to be in a nonlocomotive state when the total displacement in the abscissa and ordinate of the front LED did not exceed 2 pixels in successive positions (Fig. 4A). Positional displacements not fulfilling the above criterion were categorized as straight motion or turns based on other criteria for movement trajectories. The straight motion started with the animal entering one arm and ended with the animal completely stopping at the arm-ends (Fig. 4B). Right and left turns were characterized with semicircular trajectories at the end of each arm (Fig. 4C and D, respectively). Based upon these criteria, we then plotted the velocity profiles for each behavioral category (Fig. 5). On average, the mean linear velocities ($\pm$SD) for nonlocomotive state, straight motion, right turns, and left turns were 3.3 (± 3.2), 47.3 (± 8.5), 52.4 (± 11.5) and 54.1 (± 10.6) cm/s, respectively. The mean angular velocities for non-locomotive state, straight motion, right turns, and left turns were -2.2 (± 28.3), 2.9 (± 27.8), -296.4 (± 82.1) and 311.5 (± 76.9) °/s, respectively. The velocity cutoffs were drawn to minimize the overlapping in either linear or angular velocity of different behaviors. Additional cutoff separating low- from high-velocity straight motion was chosen so that approximately 20% of the straight-motion points fell in the low-velocity category. Based upon the linear velocity cutoff criterion, less than 0.3% of the nonlocomotive points were categorized as straight motion, whereas none of the straight motion points were classified as nonlocomotive. Based on the angular velocity cutoff, the overlapping in the angular velocity between straight motion and turns was between 0.3 and 0.5%.

Figure 6 illustrates the quantitative analysis method by showing two cells that were selective for specific movement modes, irrespective of head direction. One cell (top panels) was selective for right turns, while the other (bottom panels) was selective for straight motions. In the spot-plots (left panels), the dots represent the superimposed front-LED positions of the animals in the maze, and animals' behavioral states can be identified as characteristic trajectory patterns such as turns at the arm-ends and straight motion at each arm. Note that the robust firing (represented as circles) during right

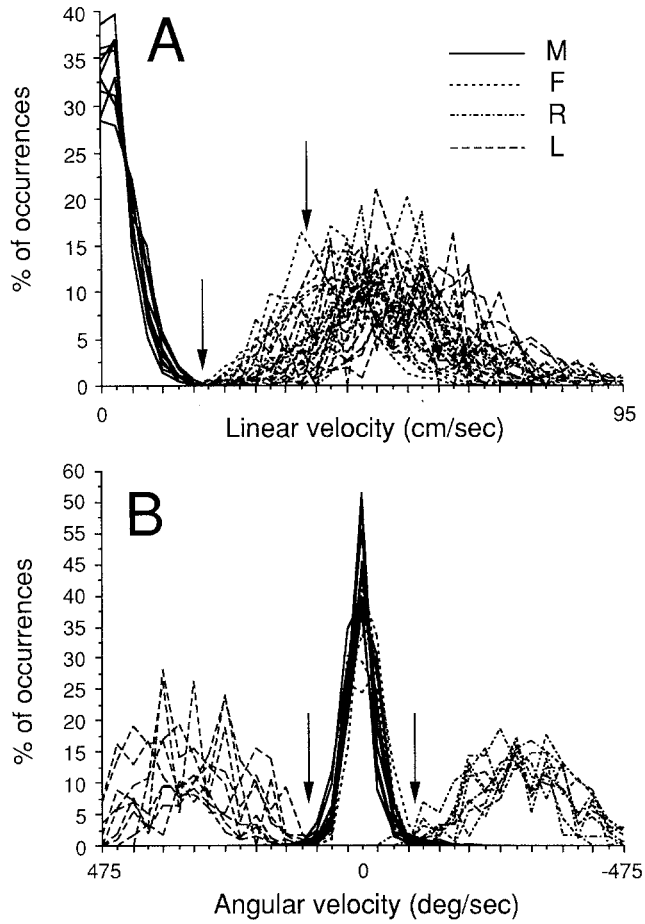

Fig. 5A,B Linear and angular velocity profiles of different behavioral modes, classified on the basis of movement trajectories in the maze, showing the velocity cutoffs used to separate different modes of motion. The ordinate represents the proportional distribution of the occurrence of behaviors separated for linear or angular velocity. The *left arrow* in **A** indicates the linear velocity cutoff between nonlocomotive (*M*) and locomotive states, whereas the *right arrow* separates the straight motion (*F*) into low-velocity and high-velocity modes. The two arrows in **B** indicate the angular velocity cutoff for right turns (*R*) and left turns (*L*). Data obtained from nine animals were superimposed on the plots

turns for the cell shown at the top and the ceased firing during all turns for the other cell are readily observed. However, the spot-plots cannot reveal the neuron's behavioral correlates while the animals are at the maze center, in which the behavioral states cannot be easily associated with either right or left turns simply based upon only the positional information of the front LEDs. In contrast, the firing profiles (right panels) can reveal neuronal correlates with distinguishable behavioral states based upon the behavioral categorization scheme. Note that the cell of the top-right panel showed a robust firing during right turns and near zero firing rate during left turns, thus confirming that some of the robust firing of this cell, shown on the maze center in the spot-plot, reflected the activity during right turns, not left turns.

Criteria and statistical analysis of the directionality of HD cells

Because the directionality of HD cells can be maintained following the removal of visual cues (Ranck 1984; Taube et al. 1990b) and the areas we studied receive extensive visual inputs, it is critical to discriminate HD cells from cue-dependent cells. HD cells were classified on the basis of either of two criteria: the cell had to exhibit significant directionality (see below), and the directionality had to be preserved in darkness or following removal of the relevant visual stimuli. Cells were classified as being cue-dependent if they exhibited a directional preference in responding to the localized visual cues, but showed no directionality in the absence of cues or in darkness (Chen et al. 1994).

Head-directional correlates were assessed by plotting the firing rate of each cell for each of eight different directions (see Figs. 5–7). Two statistical tests were applied in order to determine objectively whether the directional variance reached statistical significance. First, analysis of variance (ANOVA) was applied to determine whether these cells showed differential activities in different directions (F-test, $\alpha = 0.01$). The differential firing could be in any of the behavioral modes of any given recording session. Second, the directional tuning of these cells was tested against a uniform distribution using the Rayleigh test ($\alpha = 0.05$; Mardia 1972). After a cell passed the statistical tests, the cell was further examined for its directionality in the absence of visual cues (i.e., no-cue session of the maze task) or in total darkness to exclude the cue-dependent cells. In total, 16 cells were excluded, half (8/16) of these were simply illuminance sensitive, while the others (8/16) were visual-movement sensitive (Chen et al. 1994).

Table 1 shows the results of statistical analysis of the directional tuning of posterior cortical cells, based on the data obtained using the dual-LED tracking method. These HD cells were recorded in four animals in which 36 penetrations were made. The proportional distribution of HD cells in areas RSG (8.5%) and RSA (8.4%) was significantly higher than that in area Oc2M (2.7%; χ^2-test, $P < 0.01$ and $P < 0.02$, respectively). The trend was consistent with the probability of encountering HD cells per penetration (0.89, 1.04, and 0.32 for areas RSG, RSA, and Oc2M, respectively) in these areas, suggesting that the differential distribution of HD cells was not due to sampling bias. We conducted a quantitative comparison on the mean observed peak firing rate of these HD cells among different areas, as shown in Table 2. There was a significantly higher mean peak firing rate for the HD cells in RSG than Oc2M (Scheffee test following ANOVA, $P < 0.005$), whereas the mean peak firing rate between Oc2M and RSA and that between RSA and RSG were not significantly different (Scheffee test, $P > 0.10$ and $P > 0.15$, respectively). Moreover, there was no significant difference in the mean peak firing rate for particular behaviors (ANOVA, $P > 0.50$). Table 3 shows a quantitative comparison of the direction selectivity for

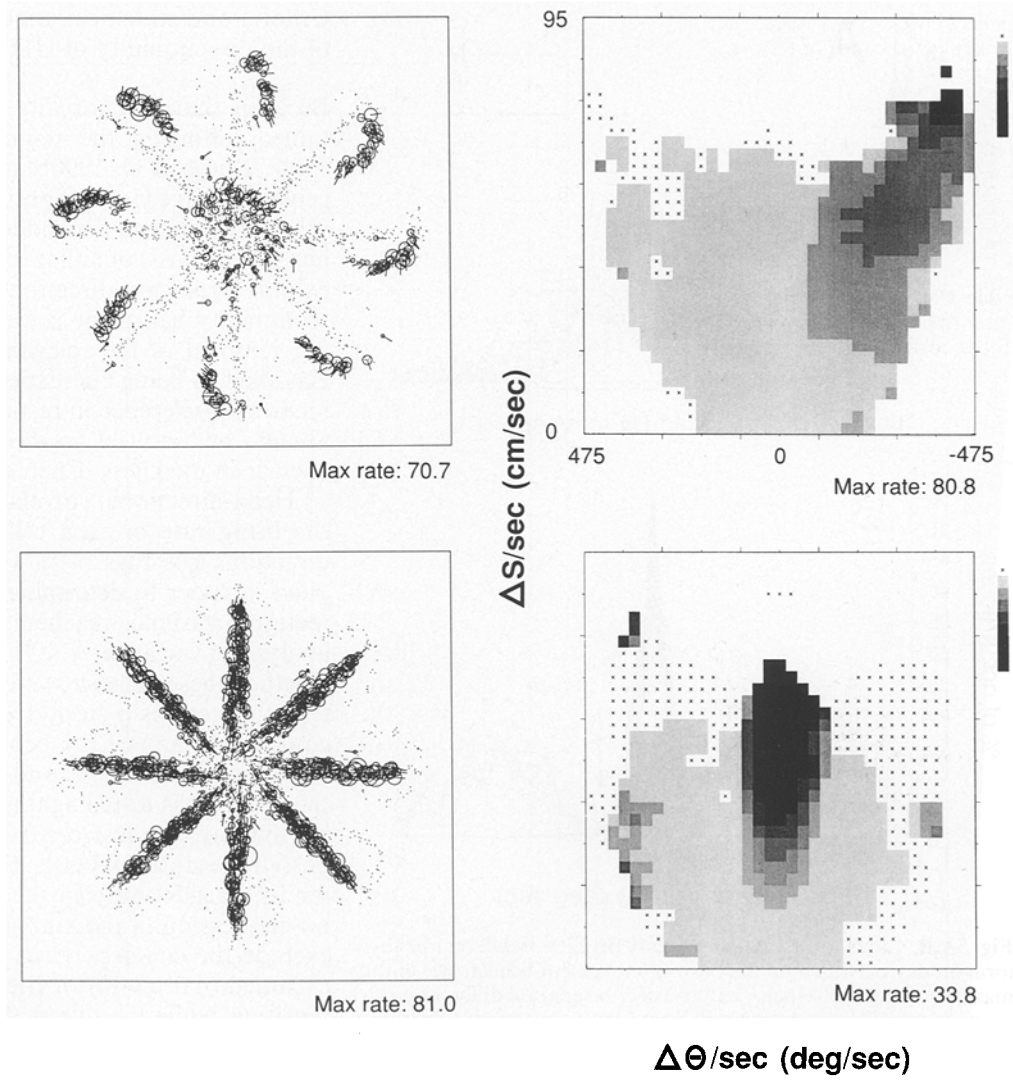

Fig. 6 Examples of two movement-selective cells in the hindlimb sensorimotor area (area HL) with their firing patterns on the maze surface illustrated in spot-plot (*left panels*) and their firing plotted against linear and angular velocities (*right panels*). In the spot-plot, each point represents the animal's position within a local integration center (5 pixels in radius) on the maze surface. The locally computed firing rate (*circles* that are scaled in proportion to the cell's maximum firing rate) and head directions (*vectors*) are superimposed as the cell consistently fired each time the animals traversed through the same location. In the firing profiles, the firing rate of the cell is represented by *gray pixels*, as in Fig. 3B, and *x* is indicative of zero firing rate

Table 1 Distribution of head-direction (*HD*) cells across cortical areas. The statistics were based on the data obtained in the second group of animals recorded using the dual-light-emitting diode tracking method

Cells	Oc2M	RSA	RSG	Total (*n*)
Total (*n*)	257	311	94	662
F-test: significant at $P<0.01$				
Number	22	43	11	76
Percentage	8.6	13.8	11.7	11.5
Rayleigh: significant $P<0.05$				
Number	16	32	9	57
Percentage	6.2	10.3	9.6	8.6
Cue-dependent[a] (*n*)	9	6	1	16
HD cells				
Number	7	26	8	41
Percentage	2.7	8.4	8.5	6.2
Behavior-selective HD cell				
Number	4	5	0	9
Percentage of HD cells	57.1	19.2	0	22.0

[a] These cells exhibited no directionality in the absence of visual cues or in the dark

these HD cells among different areas. The direction selectivity index is calculated as a ratio of the firing rate at the preferred direction over that at the null direction (i.e., 180° away from the preferred direction). There was no statistically significant difference in the direction selectivity index among different areas separated for the behavioral modes (nonlocomotive, right turn, left turn, high-speed straight motion, low-speed straight motion; Kruskal-Wallis test, $P>0.05$, $P>0.20$, $P>0.10$, $P>0.10$, and $P>0.10$, respectively). Neither was the

Table 2 Mean peak firing rate (spikes per second) of head-direction (*HD*) cells across cortical areas. (*M* nonlocomotive, *R* right turn, *L* left turn, *H* high-speed straight motion, *O* low-speed straight motion)

Cortical area	HD cells-(*n*)	M		R		L		H		O	
		Mean	SEM	Mean	SEM	Mean	SEM	Mean	SEM	Mean	SEM
Oc2M	7	8.7	1.6	12.0	2.6	10.5	1.9	9.6	1.5	11.7	1.8
RSA	26	16.1	2.5	19.5	4.2	19.0	4.5	17.6	3.4	17.3	3.2
RSG	8	22.6	4.9	24.3	5.9	25.6	6.4	23.0	4.7	23.5	5.3

Table 3 Mean directional selectivity indices of HD cells across cortical areas. (*M* nonlocomotive, *R* right turn, *L* left turn, *H* high-speed straight motion, *O* low-speed straight motion)

Cortical area	HD cells-(*n*)	M		R		L		H		O	
		Mean	SEM	Mean	SEM	Mean	SEM	Mean	SEM	Mean	SEM
Oc2M	7	5.4	1.1	5.4	1.3	14.5	5.1	6.4	2.7	5.8	2.6
RSA	26	3.4	0.8	4.3	1.4	3.5	0.9	7.7	3.8	3.4	0.9
RSG	8	6.0	4.5	5.9	4.3	6.2	4.4	3.2	1.6	3.3	1.7

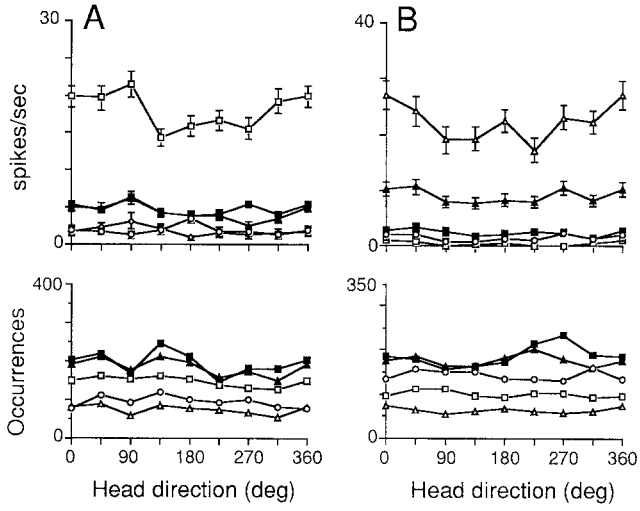

Fig. 7A,B Examples of the directional tuning curves (*upper panels*) of the two non-head-direction cells in Fig. 6; cells categorized on the basis of different modes of motion. The relative occurrences of the various motions are indicated in the lower *panels*. (—■— Nonlocomotive, —▲— low-speed straight motion, —□— right turn, —△— high-speed straight motion, —○— left turn)

mean direction selectivity significantly different among the behavioral modes (Friedman test, $P > 0.06$).

Behavioral modulation on the HD cells

To assess the influence of behavioral state on each cell's firing characteristics, we compared the activity of the cell during each behavior with that occurring when the animal was in the nonlocomotive mode. Cells were classified as behaviorally selective if they exhibited significantly increased or decreased activity during a particular behavioral state, relative to the nonlocomotive state. Two examples of movement-selective, non-HD cells that fulfilled these criteria are illustrated in Fig. 7. Cell A showed significantly increased activity during right turns, whereas cell B showed a significant increase in activity during high-velocity straight motion, with less activity during low-velocity straight motion. Examples of HD cells with and without behavioral selectivity are illustrated in Fig. 8. Cells A, B, and C showed differential firing when the animals faced particular directions. These cells, however, exhibited differing degrees of behavioral modulation: cell A was not behaviorally selective; cells B and C were behaviorally selective, and both were most active during right turns toward the preferred direction (*t*-test, $P < 0.005$ at 0° for B; $P < 0.001$ at 225° for C). However, their activities were relatively suppressed at the preferred direction for the other behavioral modes, compared with the firing rate during the nonlocomotive mode. The activity of cell B was suppressed during left turns (*t*-test, $P < 0.025$ at 0°), and to a lesser extent, during high-velocity straight motion ($P < 0.040$ at 0°). Cell C showed similar suppression during left turns ($P < 0.001$ at 225°) and high-velocity straight motion ($P < 0.025$ at 225°). The behavioral selectivity often included more than one type of behavioral mode. The interaction between the behavioral selectivity and the directional firing was either nonlinear (Fig. 8B) or linear (Fig. 8C). In the case of linear interactions, the cell showed raised activity in all directions for particular behavior modes, suggesting an additive relationship between behavioral correlates and head-directional correlates. In the case of nonlinear interactions, behavioral modulation was only present at or near the preferred direction (e.g., Fig. 8B). All behaviorally selective HD cells showed some significant directional firing in the non-locomotive mode.

Of all (41) HD cells identified, 9 cells were sensitive for behavioral mode; these cells were found in areas Oc2M ($n = 4$) and RSA ($n = 5$; Table 1). However, none of the HD cells in the RSG were behaviorally selective. The proportion of the behavior-modulated HD cells differed significantly between areas Oc2M (57%) and RSA (19%; χ^2-test, $P < 0.05$), suggesting there may exist a functional parceling among the posterior cortices.

Figure 9 illustrates modulation index plots for the nine behaviorally selective HD cells. Each modulation

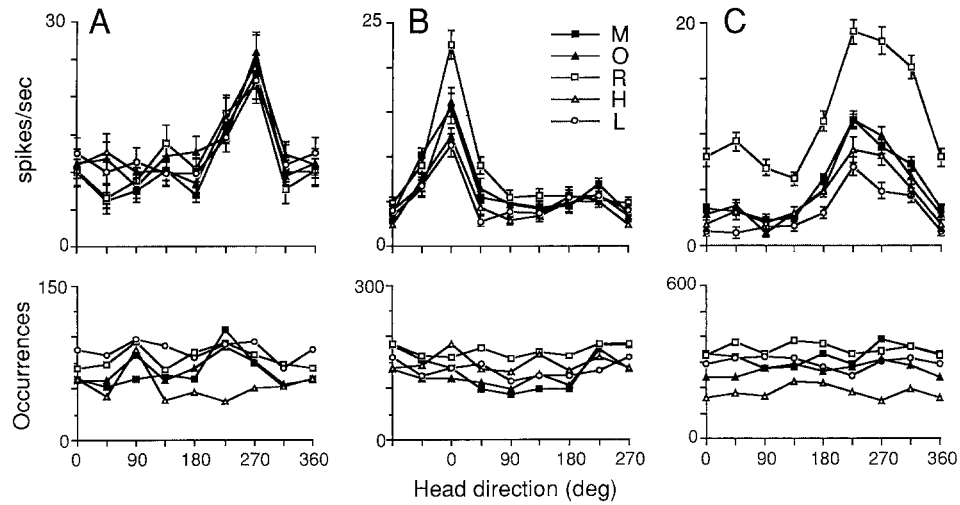

Fig. 8A–C Examples of directional tuning curves separated for different modes of motion (*upper panels*) and the corresponding occurrences for each behavior (*lower panels*) in three head-direction cells. Cell **A** (recorded in dysgranular retrosplenial cortex, RSA) was not selective for behavioral modes, whereas **B** cell B (recorded in RSA) and **C** cell C (recorded in medial prestriate cortex, Oc2M) were modulated selectively. (The *abbreviations* for different modes of motion are the same as in Fig. 7)

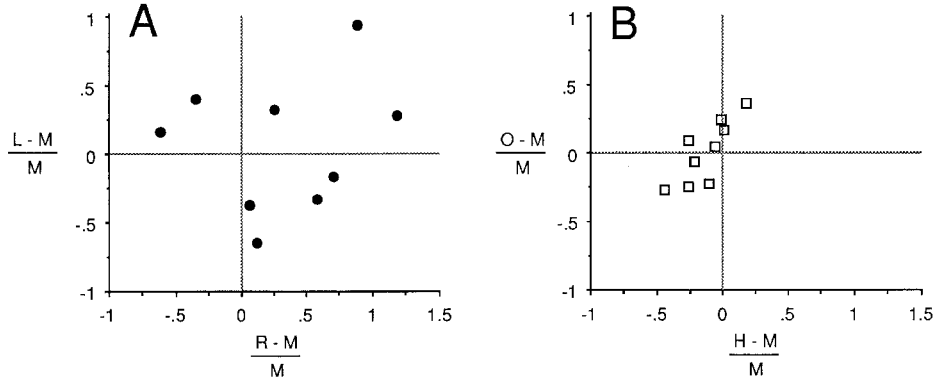

Fig. 9A,B Behavioral modulation index plots of the behaviorally selective head-direction (HD) cells indicating differential modulation for different modes of motion. Each *dot* represents a HD cell with its right-turn modulation index plotted against its left turn modulation index (**A**) or with its high-velocity straight motion modulation index plotted against low-velocity straight motion modulation index (**B**). *R*, *L*, *H*, *O*, and *M* represent the firing rate at the cell's preferred direction for right turns, left turns, high-velocity straight motion, low-velocity straight motion, and non-locomotive state, respectively

index was formulated as $(B–M)/M$, in which B represented the firing rate in the cell's preferred direction for a given behavioral mode and M represented that for non-locomotive mode. The dots plotted for turn modulation indices are scattered apart (Fig. 9A), whereas the dots plotted for straight motion modulation indices are clustered around zero (Fig. 9B). The absolute values of the turn modulation index were significantly higher than those of the straight motion modulation index (Mann-Whitney U-test, $P<0.002$), suggesting that the behavioral modulation was much stronger for turns than straight motions. There was no significant difference in the absolute value of the index between right and left turns (Mann-Whitney U-test, $P>0.60$) or between high-velocity and low-velocity straight motions ($P>0.63$). We also found no significant difference in either of the indices between areas Oc2M and RSA (Mann-Whitney U-test, $P>0.50$). The absolute values ($\pm$SD) of the behavioral modulation indices in Oc2M for right turns, left turns, high-velocity straight motion, and low-velocity straight motion were 0.65 ($\pm$0.39), 0.28 ($\pm$0.08), 0.11 ($\pm$0.11), and 0.13 ($\pm$0.08), respectively; whereas those in RSA were 0.42 ($\pm$0.36), 0.51 ($\pm$0.30), 0.22 ($\pm$0.16), and 0.24 ($\pm$0.11), respectively.

Simultaneously recorded HD cells

We noted that HD cells were sometimes recorded simultaneously in the same penetration, although HD and non-HD cells were often recorded together in pairs or in adjacent recordings. The HD cells recorded simultaneously appeared to have preferred directions that were either similar ($\pm$45°) or complementary ($\pm$180°) to each other. In the present study, three groups of two to three HD cells were found in the recordings of three different animals. In two (one in Oc2M and one in RSA) out of the three groups, three HD cells were recorded simultaneously; two of these cells showed similar preferred directions, and the third cell exhibited a directional preference which was complementary to that exhibited by the other two cells in the group. In another HD cell cluster recorded in area RSA, one pair of two HD cells showed complementary preferred directions.

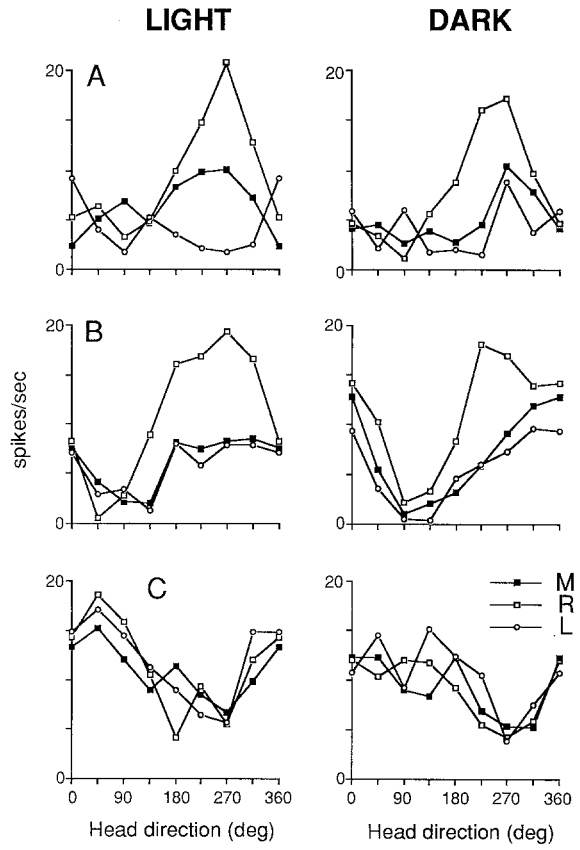

Fig. 10A–C Directional tuning of three HD cells simultaneously recorded in the medial prestriate cortex (area Oc2M), showing persistent directional preferences and behavioral correlates in both light and dark conditions. The *left panels* show the spatial tuning data during a test at the center of the maze under conditions of normal illumination, while the *right panels* illustrate data from the same cells in total darkness. The average spike heights and widths (mean ±SD) were 139±18 μV, 477±76 μs; 148±16 μV, 217±22 μs; and 78±11 μV, 522±128 μs for cells A (**A**), B (**B**), and C (**C**), respectively

Figure 10 illustrates examples of three HD cells that were simultaneously recorded when the animals searched for food on the central platform of the maze. Cells A and B showed the most robust directional firing at 270°, whereas cell C was tuned to 45°. These simultaneously recorded HD cells, however, did not necessarily show similar behavioral selectivity. Cells A and B exhibited significantly increased firing during right turns in the preferred directions (270°; *t*-test, $P<0.025$ and $P<0.001$, respectively), compared with the firing in the nonlocomotive mode. However, cell C was not selective for behavioral modes. These results suggest that behavioral selectivity can be decoupled from the directional firing in adjacent cells. The same cells were tested in total darkness (right panels in Fig. 10), and their preferred directions and behavioral selectivities were similar to those in the light. That the presence or absence of light had little effect on the apparent behavioral selectivity of these cells suggests that the behavioral selectivity is not visually driven. We conducted an additional test by rotating the central platform and found that the rotation of the platform affected neither the directional firing nor the behavioral selectivity of these cells. This result rules out a possible contribution of local cues (e.g., urine marks) for the directional preference or the behavioral selectivity of these cells. Thus, the behavioral modulation on these HD cells is unlikely to result from a passive response to external sensory inputs, but rather from internal movement information.

Discussion

The major finding of this study was that HD cells are widely distributed in the posterior cortex, including areas Oc2M, Oc2L, RSA, and RSG. These data provide additional evidence suggesting that those areas participate in spatial information processing regarding head directions. We also found that associations between movement and directionality exist in a high proportion of HD cells in the Oc2M and in a small proportion of those in the RSA, whereas there was no apparent behavioral modulation of the directional firing in the HD cells recorded in area RSG.

Quantitative method for behavioral categorization

Previous behavioral analyses of freely moving animals have generally been limited to position detection using the single-LED tracking method (O'Keefe 1979; McNaughton et al. 1983; Muller et al. 1987; Eichenbaum et al. 1987). Some forms of movement analyses have been attempted by using the movement vectors that are derived from animals' positions in time sequence (Wiener et al. 1989; McNaughton et al. 1986). Wiener et al. (1989) created a turning index by measuring the angles subtended from the vectors which were drawn from the target point to the previous and subsequent points in 200-ms time frames. As they have pointed out, this index only measures the movement of animals' head positions rather than true head rotation. That is, nonturning movements with angular trajectory of head positions can be confused with actual head rotation. In addition, other nonlocomotive behaviors, such as grooming, can be categorized as fast right or left turns if the video-images of single LED points moved back and forth between neighboring locations. Therefore, this method is not suitable for a quantitative behavioral classification. The method of McNaughton et al. (1986) takes advantage of the characteristic behaviors on the radial-arm maze, in that movement trajectories of rats on the maze form unique patterns (see Figs. 4, 6). Turns are made as semicircular trajectories at the arm-ends, while straight motions occur in the middle of each arm. Thus, each behavior is separated based on the maze geometry. However, this advantage is limited to some behaviors in part of the maze. Thus, the technical constraints of the single-LED tracking method limit the extent of behavioral analyses.

The dual-LED tracking method offers four major advantages over other methods of tracking position. First, head directions can be inferred from the front-back LED alignments. Because head directions are derived from the animals' head-neck orientation, a change of head-direction vectors then represents actual turning behaviors (see Fig. 3A). Second, animals' head direction and behavioral states can be measured simultaneously, allowing a direct comparison between the two variables. Third, virtually all planar behaviors can be objectively analyzed using this method, regardless of geographical constraints of the recording apparatuses. Finally, some non-task-related behaviors can be excluded from behaviors of interest. For example, grooming behaviors, characterized as movements of high angular velocity and low linear velocity, can be identified and excluded from the analyses (see Fig. 3B). Also, nonplanar behaviors (e.g., pitch) can be excluded, because the front-back LED arrays would be fused together in this case. It is important to point out that, in the present study, the "nonlocomotive" state was defined as a behavior in which there was little movement in either the linear or angular plane. This state included behaviors such as drinking chocolate milk, resting, sleeping, or chewing food pellets. These states were undifferentiable by our analysis. In addition, the behavioral analysis method used in this study provides no information about some unique behaviors, such as trunk or limb movements, which might have had some influence on the activity of the cells recorded.

Motor versus sensory role of the behavioral correlates of HD cells

There is a general issue concerning the motor or sensory nature of the behavioral selectivity in HD cells. The extreme motor hypothesis would argue that behavioral selectivity reflects a motor command which orients the animals toward specific directions. If this were true, motor behaviors would be required to cause HD cells to fire. However, we found that all HD cells exhibited a directional firing in the nonlocomotive modes, suggesting that the behavioral correlates are unlikely to be simply a reflection of motor commands. This conclusion is consistent with results from a previous study, in which it was demonstrated that postsubicular HD cells maintained directionality, albeit with somewhat lower signal-noise ratios, when the animals were hand held (Taube et al. 1990b). These results together argue against the "goal-directed" motor command hypothesis, but do not rule out a modulatory role of motor efference-copy.

An alternative hypothesis is that the behavioral correlates may be induced by visual motion which occurs in parallel with the animal's movement. This possibility is ruled out by the fact that HD cells were able to maintain their behavioral selectivity in total darkness (see Fig. 9). We cannot rule out the influence of other nonvisual cues, such as vestibular or proprioceptive inputs, which occur simultaneously while the animals are in motion in total darkness (Potegal 1987; Mergner et al. 1991). These sensory inputs may contribute to the behavioral correlates of HD cells, and their role remains to be elucidated in further studies.

Behavioral modulation of directional firing

The finding that some HD cells were behaviorally selective provides direct physiological evidence that an integration of movement and directional information exists in spatial information processing. The integration of movement information is probably important for maintaining a directional constancy (Mittelstaedt and Mittelstaedt 1980; Gallistel 1990). For example, when we rotate ourselves through 360°, we retain a clear sense of being oriented in the original direction, even in the dark. Observations like this one point out that we are capable of tracking self-movements, such that the direction sense is updated instantaneously.

Information regarding changes in an organism's direction are undoubtedly critical for maintaining an internal representation of head direction. Turning is one of the most important modes of motion that conveys information regarding changes in one's direction. Thus, it is likely that turn-selective HD cells may be involved in the neural circuit which updates the internal representation of head orientation, given that the cells simply track the angular displacements in respect to the previous head direction (McNaughton et al. 1991). The results in Fig. 10, showing that the behavioral modulation persisted in total darkness, are consistent with this hypothesis, suggesting that the internal movement information was sufficient to support the directional firing of HD cells, irrespective of the existence of external visual inputs. Updating the current directional representation requires information of the previous head orientation and the on-going action that leads to a change of direction. Therefore, the finding that there exists an integration of changes of head orientation and current head direction provides a plausible computational basis for generating an updated (and possibly predicted) representation of head orientation (McNaughton et al. 1991; Chen et al. 1994). Similar neuronal properties have been found in other cortical areas, such as motor cortex (Georgopoulos et al. 1989) and posterior parietal cortex (Duhamel et al. 1992), in which neurons not only track the current spatial coordinates of the arm or eye but also predict the upcoming spatial coordinates on the basis of the movement information. Our finding that movement information is involved in the directional processing is consistent with results from these studies.

We found in this study that the spatial firing of some HD cells was modulated by non-angular movements such as straight motion, although the modulation was much less robust than that achieved by angular movements (Figs. 2, 8 9). The data thus suggest that the non-

angular movements may also be involved in directional processing. Unlike angular movements, which primarily change head orientation but not positions, the nonangular movements change little of head orientation but primarily carry animals from one place to another. Thus, incorporation of nonangular movements into the directional representation may be important for carrying the directional information over long distances, such that one can maintain a consistent sense of direction regardless of location in a given environment. This explanation may account for the "location-invariant" nature of the preferred directions of HD cells (Ranck 1984; Taube et al. 1990a).

The contribution of egocentric movement to spatial processing has been extensively studied in oculomotor systems (Robinson 1973; Mountcastle et al. 1975; Andersen et al. 1990; Sparks and Mays 1990). In the posterior parietal cortex, cells are tuned to neither sensory (retinal) nor motor (position of the eyes in orbit) coordinates. Rather, most spatially tuned cells code a conjunction of retinal and eye position signals, suggesting that the final spatial coding of these neurons results in an integrated "head-centered" coordinate (Andersen et al. 1990; Zipser and Andersen 1988). Our finding that there exists an integration of motion (motor coordinate) and head-directionality (angular coordinate) appears to be in line with this general scheme of spatial coding, suggesting that such an integration may result in a coding of allocentric coordinates that is independent of self-movement (McNaughton et al. 1991).

The role of neocortex and periallocortex in head-direction processing

Our results indicated that the behavior-selective direction cells were all localized in part of the neocortex (Oc2 and RSA), implying that the neocortex may be important in tracking movements. The rostral portion of area Oc2M in rodents is thought to be the homolog of the posterior parietal cortex in primates, based on anatomical and sensory-evoked mapping evidence (Krieg 1946; Vogt and Miller 1983; Miller and Vogt 1984; Kolb and Walkey 1987; Toldi et al. 1986; Miller 1987). The finding that the Oc2M was primarily involved in behavioral selectivity of the head directional processing implies that this part of the neocortex, similar to its counterpart in the primate posterior parietal cortex (Mountcastle et al. 1975; Andersen 1987), is important in higher-order spatial processing.

In the present study, there was a trend for a slight increase in the mean peak firing rate of the HD cells in part of the retrosplenial cortex, RSG, in comparison with those in the Oc2M (Table 2). Whether the difference in the peak firing rates reflects any functional difference among these areas remains to be investigated in future studies. The HD cells recorded in other brain regions, such as striatum (Wiener 1993) and postsubiculum (Taube et al. 1990a), have been shown to have a wide range of peak firing rates, ranging from 4 to 120 spikes/s. Thus, it would be unlikely that a relative difference in the peak firing rate is associated with any particular function of an area as a whole. Moreover, we have found no regional difference in the directional selectivity for the HD cells between the neocortex and periallocortex (Table 3), suggesting that the head directional information is well conserved through the cascade projections from the neocortical areas to the limbic areas.

The only noticeable difference in the property of the HD cells in different brain regions is the directional tuning width. The striatal HD cells seem to show relatively broad directional tuning (about 160–220°), which is similar to that of some neocortical HD cells reported in the present study, but is dissimilar to the sharply tuned HD cells in postsubiculum (Taube et al. 1990a). However, some HD cells recorded in the present study did show narrow directional tuning, similar to that in the postsubiculum. It is thus unclear whether the difference of directional tuning width reflects any physiological significance. Note that these reports have been conducted using different methodologies, including different recording apparatuses, trained behaviors, and cue manipulations (also see Discussion in Chen et al. 1994). It would not be surprising to find interstudy differences in some of the data parameters, such as firing rate and directional tuning. This issue is beyond the scope of the present study and should be thoroughly investigated in future studies.

In a previous study, Taube et al. (1990a) observed that some HD cells recorded in the postsubiculum showed a slight preference for either clockwise or counterclockwise rotations, suggesting that the information about movement may also reach part of the periallocortex. However, such behavioral modulation was quite infrequent in the postsubiculum, as Taube et al. (1990b) identified only 2 of 25 HD cells with this property. Thus, behavioral modulation may be significantly stronger in the neocortex than the periallocortex. On the other hand, the present results indicate that the HD cell proportion is higher in the periallocortex than the neocortex. This trend is consistent with the results of Taube et al. (1990a) in which a relatively high proportion (26%) of HD cells was found in the postsubiculum.

Our results, together with those of Taube et al. (1990a), suggest that the neocortex may emphasize the integration of information about movement and head-directionality, and the periallocortex emphasizes abstract and movement-independent directionality (Fig. 11). This dichotomous view of the spatial function of neocortex and periallocortex is in general agreement with the anatomical parceling of the two cortices. Phylogenetically, areas Oc2M and RSA are part of the neocortex, while area RSG and postsubiculum are part of the periallocortex (Zilles 1985). Areas Oc2M and RSA share similar thalamocortical inputs and corticocortical connections, whereas the thalamocortical and corticocortical connections of area RSG are similar to those of postsubiculum (Zilles 1985; Sripanidkulchai

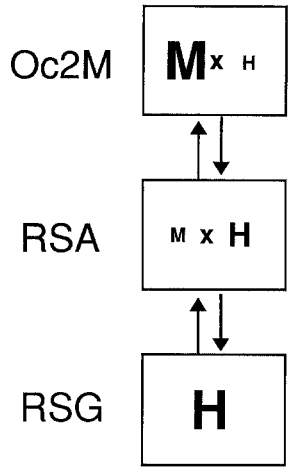

Fig. 11 Scheme reflecting the anatomical relations among the posterior cortical areas evaluated in these experiments. The relative predominance of motion (*M*) and head direction (*H*) information is indicated by the letter size. (*Oc2M* medial prestriate cortex, *RSA* dysgranular retrosplenial cortex, *RSG* granular retrosplenial cortex)

and Wyss 1986; van Groen and Wyss 1990a). Differences between the neocortex and periallocortex also appear in the anatomical connections between the two cortices. For instance, the visual cortices Oc1 and Oc2M project to the retrosplenial cortex and postsubiculum in a cascade manner (Vogt and Miller 1983; Miller and Vogt 1984; van Groen and Wyss 1990a,b). However, Oc2M receives feedback from the adjacent neocortex (e.g., RSA), but not from periallocortex such as RSG and postsubiculum (van Groen and Wyss 1990a). In contrast, the postsubiculum reciprocally connects with the RSG, but not the RSA or Oc2M (van Groen and Wyss 1990b). Thus, the patterns of cross talk among the regions also distinguish the neocortex from the periallocortex. Figure 11 illustrates the simplified anatomical connections that encompass the cascade nature of the interconnections between these areas. The relative loading of movement information processing in relation to the head-directional information processing is expressed in each area accordingly. This, in agreement with primate neurophysiological studies, suggests that the neocortex may be important in carrying out sensorimotor associations, possibly mediating sensory-to-motor spatial coordinate transformation (Andersen 1987; Sparks and Mays 1990). The periallocortex, which is heavily connected with the hippocampal formation, may participate in higher-order spatial processing, such as information about allocentric direction and location that is encoded in the neurons of the hippocampal formation (O'Keefe and Dostrovsky 1971; McNaughton et al. 1983; Ranck 1984; Muller et al. 1990).

Functional organization of local HD cells

In this study, we found that the HD cells were often recorded together with non-HD cells in the same penetration. However, HD cells which were encountered infrequently were sometimes recorded in pairs. This observation suggests that HD cells form clusters. Furthermore, the simultaneously recorded HD cells often preferred similar or complementary directions (Fig. 10), suggesting that a functional coupling may exist in local HD cells through a mechanism of reciprocal excitation or inhibition. One may argue that the complementary direction preference may result from recording artifact, such as the sampling limitations of recording equipment. It is possible that a recording of several high-rate cells simultaneously may hamper a correct spike count of other low-rate cells. If this were the case, complementary coding should be found in both behavioral selectivity and spatial tuning. However, this possibility is ruled out by our finding that the behavioral selectivity was dissociated from the directional firing of the neighboring HD cells recorded simultaneously (Fig. 10). This result also indicates a complex integration of information regarding head direction and movement.

It has been found that middle temporal (MT) cortex neurons with a similar direction of motion preference are organized in vertical columns; cells in the adjacent columns of the same axis of motion show complementary direction preference (Van Essen et al. 1981; Albright et al. 1984). Also, direction selective neurons are often surrounded by nondirectional neurons. The similarity of the findings between the motion-sensitive cells in MT and HD cells in posterior cortices suggests that the functional organization of HD cells may be similar to that of motion-sensitive neurons in area MT.

Acknowledgements We thank Dr. S. Wise for critical reading of the manuscripts; Dr. L. Harvey for helping in illuminance measurement; M. Williams, W. Skaggs, E. Ortiz, and D. Gibbons for programing and experimental assistance. This work was presented to the University of Colorado in partial fulfillment of the requirements for the PhD degree. The work was supported by PHS grant NS20331 to B.L.M. and MH 00897 to C.A.B.

References

Albright TD, Desimone R, Gross CG (1984) Columnar organization of directionally selective cells in visual area MT of the macaque. J Neurophysiol 51:16–31

Andersen RA (1987) Inferior parietal lobule function in spatial perception and visuomotor integration. In: Plum F (ed) Higher functions of the brain. (Handbook of physiology, sect 1, The nervous system, vol V, part 2) American Physiological Society, Bethesda, MD

Andersen RA, Essick GK, Siegel RM (1985) Encoding of spatial location by posterior parietal neurons. Science 230:456–458

Andersen RA, Bracewell RM, Barach S, Gnadt JW, Fogassi L (1990) Eye position effect on visual, memory, and saccade-related activity in areas LIP and 7a of macaque. J Neurosci 10:1176–1196

Chen LL, McNaughton BL (1988) Spatially selective discharge of vision and movement modulated posterior parietal neurons in the rat. Soc Neurosci Abstr 14:818

Chen LL, McNaughton BL, Barnes CA, Ortiz ER (1990) Head-directional and behavioral correlates of posterior cingulate and medial prestriate cortex neurons in freely-moving rats. Soc Neurosci Abstr 16:441

Chen LL, Lin L-H, McNaughton BL, Barnes CA, Gibbons DF (1991) Progressive decrease of behavioral modulation of head-direction cells from medial prestriate cortex to retrosplenial cortex. Soc Neurosci Abstr 17:1395

Chen LL, Lin L-H, Barnes CA, McNaughton BL (1994) Head-direction cells in the rat posterior cortex. II. Contributions of visual and ideothetic information to the directional firing. Exp Brain Res 101:24–34

Duhamel JR, Colby CL, Goldberg ME (1992) The updating of the representation of visual space in parietal cortex by intended eye movements. Science 255:90–92

Eichenbaum H, Kuperstein M, Fagan A, Nagode J (1987) Cue-sampling and goal-approach correlates of hippocampal unit activity in rats performing an odor-discrimination task. J Neurosci 7:716–732

Gallistel CR (1990) The organization of learning. MIT press, Cambridge, MA

Gallyas F (1979) Silver staining of myelin by means of physical development. Neurol Res 1:203–209

Georgopoulos AP, Lurito JT, Petrides M, Schwartz AB, Massey JT (1989) Mental rotation of the neuronal population vector. Science 243:234–236

Groen T van, Wyss JM (1990a) The postsubicular cortex in the rat: characterization of the fourth region of the subicular cortex and its connections. Brain Res 529:165–177

Groen T van, Wyss JM (1990b) Connections of the retrosplenial granular A cortex in the rat. J Comp Neurol 300:593–606

Hyvarinen J (1982) The parietal cortex of monkey and man. Springer, Berlin Heidelberg New York

Kolb B, Walkey J (1987) Behavioral and anatomical studies of the posterior parietal cortex in the rat. Behav Brain Res 23:127–145

Krieg WJS (1946) Connections of the cerebral cortex. I. The albino rat: A. Topography of the cortical areas. J Comp Neurol 84:221–275

Mardia KV (1972) Statistics of directional data. Academic, New York

McNaughton BL, Barnes CA, O'Keefe J (1983a) The contributions of position, direction, and velocity to single unit activity in the hippocampus of freely-moving rats. Exp Brain Res 52:41–49

McNaughton BL, O'Keefe J, Barnes CA (1983b) The stereotrode: a new technique for simultaneous isolation of several single units in the central nervous system from multiple unit records. J Neurosci Methods 8:391–397

McNaughton BL, Green EJ, Mizumori SJY (1986) Representation of body-motion trajectory by rat sensory-motor cortex neurons. Soc Neurosci Abstr 12:260

McNaughton BL, Chen LL, Marcus EJ (1991) "Dead Reckoning", landmark learning, and the sense of direction: a neurophysiological and computational hypothesis. J Cogn Neurosci 3:190–202

Mergner T, Siebold C, Schweigart G, Becker W (1991) Human perception of horizontal trunk and head rotation in space during vestibular and neck stimulation. Exp Brain Res 85:389–404

Miller MW, Vogt BA (1984) Direct connections of rat visual cortex with sensory, motor, and association cortices. J Comp Neurol 226:184–202

Mittelstaedt ML, Mittelstaedt H (1980) Homing by path integration in a mammal. Naturwissenschaften 67:566

Motter BC, Mountcastle VB (1981) The functional properties of the light-sensitive neurons of the posterior parietal cortex studied in walking monkeys: foveal sparing and opponent vector organization. J Neurosci 1:3–26

Mountcastle VB, Lynch JC, Georgopoulos A, Sakata H, Acuna C (1975) Posterior parietal association cortex of the monkey: command function for operations with extrapersonal space. J Neurophysiol 38:871–908

Muller RU, Kubie JL, Ranck JB (1987) Spatial firing patterns of hippocampal complex-spike cells in a fixed environment. J Neurosci 7:1935–1950

Muller RU, Kubie JL, Bostock EM, Taube JS, Quirk GJ (1991) Spatial firing correlates of neurons in the hippocampal formation of freely moving rats. In: Paillard J (ed) Brain and space. Oxford University Press, Oxford, pp 296–333

O'Keefe J (1979) A review of the hippocampal place cells. Prog Neurobiol 13:419–439

O'Keefe J, Dostrovsky J (1971) The hippocampus as a spatial map: preliminary evidence from unit activity in the freely-moving rat. Brain Res 34:171–175

Olton DS, Samuelson RJ (1976) Remembrance of places: spatial memory in rats. J Exp Psychol Anim Behav Process 2:97–116

Potegal M (1987) The vestibular navigation hypothesis: a progress report. In: Ellen P, Thinus-Blanc C (eds) Cognitive processes and spatial orientation in animal and man, vol II. Nijhoff, Dordrecht

Ranck JB (1984) Head-direction cells in the deep cell layer of dorsal presubiculum in freely moving rats. Soc Neurosci Abstr 10:599

Robinson DA (1973) Models of the saccadic eye movement control system. Kybernetik 14:71–83

Sparks DL, Mays LE (1990) Signal transformations required for the generation of saccadic eye movements. Annu Rev Neurosci 13:309–336

Sripanidkulchai K, Wyss JM (1986) Thalamic projections of retrosplenial cortex in the rat. J Comp Neurol 254:143–165

Taube JS, Muller RU, Ranck JB (1990a) Head-direction cells recorded from the postsubiculum in freely moving rats. I. Description and quantitative analysis. J Neurosci 10:420–435

Taube JS, Muller RU, Ranck JB (1990b) Head-direction cells recorded from the postsubiculum in freely moving rats. II. Effects of environmental manipulations. J Neurosci 10:436–447

Toldi J, Foher O, Wolff JR (1986) Sensory interactive zones in the rat cerebral cortex. Neurosci 2:461–465

Van Essen DC, Maunsell JHR, Bixby JL (1981) The temporal visual area in the macaque: myeloarchiteture, connections, functional properties and topographic connections. J Comp Neurol 199:293–326

Vogt BA, Miller MW (1983) Cortical connections between rat cingulate cortex and visual, motor, and postsubicular cortices. J Comp Neurol 216:192–210

Wieland CM, Eaton RC (1983) An electronic cine camera system for the automatic collection and analysis of high-speed movement of unrestrained animals. Behav Res Methods Instr 15:437–440

Wiener SI (1993) Spatial and behavioral correlates of striatal neurons in rats performing a self-initiated navigational task. J Neurosci 13:3802–3817

Wiener SI, Paul CA, Eichenbaum H (1989) Spatial and behavioral correlates of hippocampal neuronal activity. J Neurosci 9:2737–2763

Zilles K (1985) The cortex of the rat: a stereotaxic atlas. Springer, Berlin Heidelberg New York

Zipser D, Andersen RA (1988) A back-propagation programmed network that simulates response properties of a subset of posterior parietal neurons. Nature 331:679–684